AUTOMATIC DETECTION OF BOULDERS AND MEASURING THEIR SIZE AND SHAPE DISTRIBUTIONS ON RYUGU. S. Seki [1, 2], T. Kouyama[2], X. Fu[1, 2], W. Shen[1, 2] and I. Yoshikawa[1], [1]The University of Tokyo., [2]National Institute of Advanced Industrial Science and Technology.

Introduction: Size and shape distributions of boulders on asteroids give constraints on conditions of their origins and growths, which are essential for evaluating the collisional history of asteroids. In laboratory experiments, the axial ratios of fragments from catastrophic disruptions were found to be 2: $\sqrt{2}$: 1[1]. Therefore, measuring boulders can support to decide whether asteroids experienced catastrophic disruptions or not.

In research of asteroid Ryugu, because Ryugu is thought to be formed by re-accumulation after the catastrophic disruption of its parent body, boulder measurement may reveal the formation process of Ryugu. Michikami et al. [2] investigated the boulder size distributions and three-axial ratios on Ryugu by using images taken by Hayabusa2's telescopic camera (Optical Navigation Camera telescopic, ONC-T [3]). They counted about 16,000 boulders (5 cm to 7 m in diameter) that were captured in 14 close-up images (Figure 1), and concluded that the boulders were formed mainly by the catastrophic disruption of its parent body. They also found that the boulder size distributions showed a slightly different slope (power-index) in each image, suggesting different boulders inflow and formation processes in different locations.

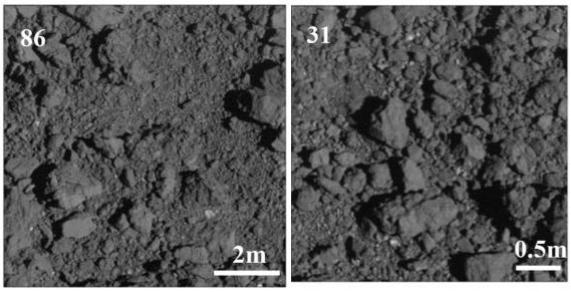

Figure 1. Examples of Ryugu close-up image [2].

The total number of close-up images by a visible band of ONC-T is ~300 that covers various locations of Ryugu, especially for the equatorial region. While analyzing surface images of the entire Ryugu and examining regional differences should be useful to reveal the formation process, Michikami et al. [2] counted boulders in just 14 images, because of a time-consuming task of counting boulders manually. Therefore, in this study, we adopt a deep learning method, the Instance Segmentation, that can not only detect boulders in an image, but also measure their shapes and sizes at the same time automatically. The goal of this study is to obtain the size distributions and three-axial ratios of the boulders and examine how regional differences emerged during the formation process of Ryugu.

Methods: This study focuses on the Instance Segmentation, that can realize "boulder detection" and "shape measurement". Since this method performs "object detection" followed by individual "region segmentation", it is suitable for detecting boulders one by one and capturing their shapes at the same time. We adopt Mask R-CNN [4] (figure 2) for the boulder detection and size measurement, which is one of the practical deep learning methods for the Instance Segmentation task. We modified the model suitable for boulder detection.

Figure 2. Examples of Instance Segmentation (Mask R-CNN [4]). Capturing contours and detecting objects individually.

Data: For the boulder instance segmentation, we used 275 close-up images taken from an altitude of 5 km or less by ONC-T. ONC-T has seven bandpass filters [3], and we used images taken with a visible wavelength band. Since we used a deep learning method, it was required to prepare appropriate and sufficient training data for the boulder detection task. We at first prepared annotations of boulders manually for training a model (Figure 3). The total number of images was 275, and the total number of boulders was about 13,000 in this study.

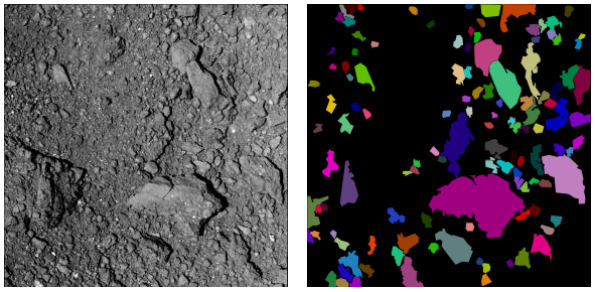

Figure 3. Examples of annotations used for training the model.

Result: We trained the Mask R-CNN model with the annotated boulders in 12 ONC-T images. The results of inference are shown in Figure 4. To obtain two-axial ratios and size distributions, we approximated the shapes of the detected boulders as ellipses. Through this procedure, we can detect boulders individually, and obtain two-axial lengths automatically, which were done manually in previous studies.

Figure 5 shows the boulder size distributions from three inference images. As in [2], the size distributions shown in figure 5 follow a power-law. In addition, while the locations of the inference images in this study are different from images used in [2], the images provided similar power indices. The power index of each image is shown in Table 1. By using the Instance Segmentation, we can detect boulders individually, and obtain the two-axial lengths automatically, which were done manually in previous studies.

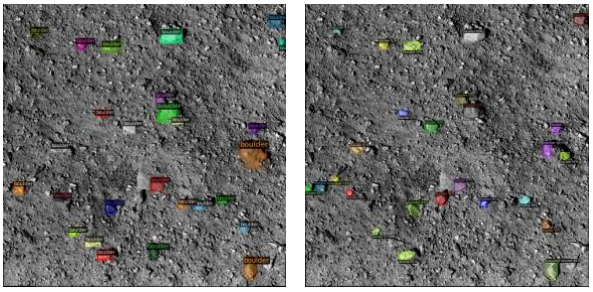

Figure 4. Training result. (Left) Ground truth. (Right) Output image.

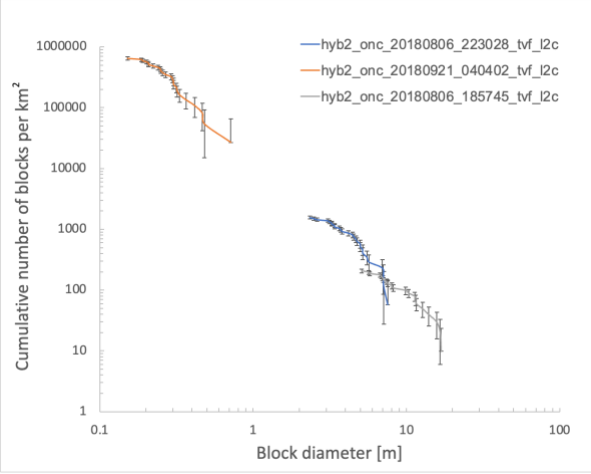

Figure 5. Boulder size distributions derived from our instance segmentation.

Table 1. The power indices of three images

Image	Power index
hyb2_onc_20180806_223028_tvf_l2c	-2.34
hyb2_onc_20180901_040402_tvf_l2c	-2.31
hyb2_onc_20180806_185745_tvf_l2c	-2.10

Conclusion: By using a deep learning method, statistics of boulders, such as size distributions and ratio of axial lengths, can be obtained automatically. Although not all boulders, especially for apparently small boulders with less than few ten pixels, have been detected yet, the resulted size distributions were consistent with those in previous studies.

We will analyze more images taken by ONC-T to investigate regional differences. We will also improve the model structure of the Mask R-CNN to detect smaller boulders. In addition, the heights of boulders can be calculated by using the lengths of boulder shadows, which can be used for evaluating the three-axial ratios [2]. We will use additional deep learning methods to detect shadows and evaluate their length in images for obtaining boulder heights automatically. For all images taken by the ONC-T, the size distribution and three-axial lengths of boulders will be automated.

References: [1] Fujiwara et al. Nature 272.5654 (1978): 602-603. [2] Michikami et al. Icarus 331 (2019): 179-191. [3] Kameda et al. Space Sci. Rev., 208 (2017): 17-31. [4] He, Kaiming, et al. Proceedings of the IEEE international conference on computer vision. 2017.